Plasma S-Nitrosothiol Status in Neonatal Calves: Ontogenetic Associations with Tissue-Specific S-Nitrosylation and Nitric Oxide Synthase

STEPHAN CHRISTEN,* ISABELLE CATTIN,† IONA KNIGHT,‡ PAUL G. WINYARD,‡ JÜRG W. BLUM,†,[1] AND THEODORE H. ELSASSER§,[2]

Institute for Infectious Diseases, University of Bern, CH-3010 Bern, Switzerland; †Division of Nutrition and Physiology, Institute of Animal Genetics, Nutrition and Housing, University of Bern, CH-3012 Bern, Switzerland; ‡Peninsula Medical School, Universities of Exeter and Plymouth, Exeter EX1 2LU, United Kingdom; and §United States Department of Agriculture, Agricultural Research Service, Growth Biology Laboratory, Beltsville, Maryland 20705

Neonatal cattle and in part neonates of other species have manyfold higher plasma concentrations of nitrite plus nitrate than mature cows and subjects of other species, suggesting an enhanced and needed activation of the nitric oxide (NO) axis at birth. While the biological half-life of NO is short (<1 sec), its functionality can be prolonged, and in many regards more discretely modulated, when it reacts with low-molecular-weight and protein-bound thiols to form S-nitrosothiols (RSNO), from which NO subsequently can be rereleased. We used the calf as a model to test the hypothesis that plasma concentrations of RSNO are elevated at birth in mammals, correlate with ascorbate and urate levels, are selectively generated in critical tissue beds, and are generated in a manner temporally coincident with changes in tissue levels of active NO synthases (NOS). Plasma concentrations of RSNO, ascorbate, and urate were highest immediately after birth (Day 0), dropped >50% on Day 1, and gradually decreased over time, reaching a nadir in mature cattle. Albumin and immunoglobulin G were identified as major plasma RSNO. The presence of S-nitrosocysteine (SNC, a validated marker for S-nitrosylated proteins), inducible NOS (iNOS), and activated endothelial NOS (eNOS phosphorylated at Ser1177) in different tissues was analyzed by immunohistochemistry in another group of similar-aged calves. SNC, iNOS, and phosphorylated eNOS were detected in liver and ileum at the earliest timepoint of sampling (4 hrs after birth), increased between 4 and 24 hrs, and then declined to near-nondetectable levels by 2 weeks of life. Our data show that the neonatal period in the bovine species is characterized by highly elevated and coordinated NO-generating and nitrosylation events, with the ontogenetic changes occurring in iNOS and eNOS contents in key tissues as well as RSNO products and associated antioxidant markers. Exp Biol Med 232:309–322, 2007

Key words: reactive nitrogen oxides; ontogenesis; S-nitrosylation; nitric oxide synthase

Introduction

For the neonate, the transition from fetal life to existence in the extrauterine world constitutes a period of intensely brittle homeostatic readjustments (1). Elevated plasma concentrations of total nitrate plus nitrite, the footprint of enhanced nitric oxide synthase (NOS)-mediated nitric oxide (NO) production from arginine (2, 3), as well as several other recent lines of evidence, suggest that the NO axis plays a critical role in the neonate's adjustments to life (4, 5). Two examples of the extent to which neonatal physiological systems are profoundly dependent on NO-directed activities are readily evident. In cardiovascular adjustments and compensation, NO controls local blood flow, which ensures adequate tissue perfusion (1, 6). Also, NO-dependent posttranslational modification, such as S-nitrosylation of proteins, serves to provide moment-to-moment control over many catalyzed reactions (7, 8). Oxidative stress has been known to develop in the neonate during the birthing process and has been associated with

This study was partially funded by the Swiss National Science Foundation (grants 32–56823.99, 32–67205.01 and 32–66845.01) and by the H.W. Schaumann Stiftung, Hamburg.

[1] Current address: Veterinary Physiology, Vetsuisse Faculty, University of Bern, CH-3012 Bern, Switzerland.

[2] To whom correspondence should be addressed at United States Department of Agriculture, Agricultural Research Service, Growth Biology Laboratory, Building 200, Room 201, B.A.R.C.-East, Beltsville, Maryland 20705. E-mail: elsasser@anri.barc.usda.gov

Received August 26, 2005.
Accepted July 31, 2006.

1535-3702/07/2322-0309$15.00

several circulatory and mitochondrial energetic problems that affect organ function. Modulation of the NO production and total antioxidant status can remediate these problems and result in a clinically favorable outcome for challenged infants (9–11).

The NO has a half-life of less than a second *in vivo* because of its propensity to rapidly react with metalloproteins (e.g., guanylate cyclase) or convert into other reactive nitrogen oxide species (12). NO reacts with low-molecular-weight or protein-bound thiols (*via* nitrosonium cation) to form S-nitrosothiols (RSNO), a reaction termed S-nitrosylation.[3] RSNO possess many of the biological properties of NO (13–16), but with a much longer biological half-life. Serum albumin constitutes the major free thiol (~0.5 m*M*) in blood plasma of mammals. The single free thiol group of bovine serum albumin (BSA), cysteine 34, is readily S-nitrosylated under physiological conditions (15, 17), yielding S-nitrosoalbumin (SNALB). The observation that SNALB is more stable than low-molecular-weight RSNO in plasma (15) led to the proposal that SNALB could serve as a physiological reservoir and circulating carrier of NO (15, 18).

Research has addressed many NO-related aspects of neonatal adaptation in the time period immediately following birth (19–21). However, there exists a gap in information regarding tissue-specific localization of S-nitrosylating activity in this period. Newborn calves are characterized by extremely high plasma levels of nitrite plus nitrate (nitrate+nitrite, the stable end products of NO) at birth that rapidly decrease in the first week of life (22), likely in a temporal concordance with increased use of substrate arginine within the urea cycle (23). A similar gap in information exists in the relationship between RSNO and antioxidant status, expressed by ascorbate and urate levels in particular. Ascorbate facilitates the release of NO from RSNO like SNALB in the presence of copper ions (24), while urate may function as a deterrent to the inopportune formation of nitrotyrosine in proteins by its ability to scavenge peroxynitrite, with the efficiency of this interaction increasing in the presence of ascorbate (25). Therefore, the objective of the present study was to determine the ontogenetic relationships between plasma concentrations of RSNO, the endogenous antioxidants ascorbate and urate, and tissue-localized components of the NO axis in the calf after birth. A scheme of the possible biochemical interactions between these different parameters is depicted in Figure 1.

[3] The expression "S-nitrosylation" indicates the addition of a nitrosonium cation equivalent (as opposed to NO radical) to another reactant to form a nitroso or nitrosyl species (8). While chemists prefer to use the term "S-nitrosation," physiologists tend towards the term "S-nitrosylation" to indicate the equivalent reaction but within a biological context (as in another modification "phosphorylation"). In this paper we use the expression S-nitrosylation to indicate post-translational modification of a protein.

Materials and Methods

Chemicals and Reagents. HiTrap Protein G HP and PD-10 (Sephadex G-25) columns were from Amersham Biosciences (Otelfingen, Switzerland); BSA, essentially fatty acid–free, from Calbiochem (La Jolla, CA); spermine NONOate from Cayman Chemicals (Ann Arbor, MI); sodium nitrite ($NaNO_2$) and sodium nitrate ($NaNO_3$) from Fluka (Buchs, Switzerland); acetonitrile (HPLC grade), copper sulfate ($CuSO_4$), metaphosphoric acid, and sodium dithionite ($Na_2S_2O_4$) from Merck (Darmstadt, Germany); *N*-[6-(biotinamido)hexyl]-3′-(2′-pyridyldithio) propionamide (biotin-HPDP) and horseradish peroxidase-conjugated neutravidin from Pierce (Rockford, IL); and dithiothreitol, reduced glutathione, methyl methanethiosulfonate (MMTS), neocuproine, S-nitroso-N-acetylpenicillamine (SNAP), S-nitrosoglutathione, and monoclonal anti-BSA from Sigma-Aldrich (St. Louis, MO). For use in Western blot analysis of S-nitrosylated proteins, antibody against S-nitrosocysteine (SNC) was procured from Sigma Biologicals, St. Louis, MO; for immunohistochemical procedures identifying SNC, antibody against SNC (rat anti-SNC) was a kind gift of Dr. H. Ischiropoulos and Dr. A. Gow, Children's Hospital of Philadelphia, University of Pennsylvania, Philadelphia, PA. Mouse monoclonal anti-phospho-eNOS (Ser1177) was from Biomol International L.P. (Plymouth Meeting, PA) and mouse monoclonal anti-iNOS from BD-Transduction Laboratories (San Jose, CA). Immunohistochemical visualization reagents were from the Vectastain-Elite anti-mouse and anti-rat avidin-biotin complex (ABC) kits (Vector Labs, Inc., Burlingame, CA).

Animals, Blood and Tissue Sampling, and Study Design. Studies with young and mature cattle were performed in accordance with the current Swiss Law on Animal Protection as approved by the Cantonal Committee for Animal Experimentation of the Canton of Freiburg (Granges-Paccot, Switzerland) or as approved by the USDA Institutional Animal Care and Use Committee, Beltsville, MD. For studies involving the measurement of plasma components (ascorbate, urate, total nitrite+nitrate, RSNO, S-nitrosylated proteins), calves and cows (Brown Swiss, Holstein-Friesian, Red Holstein) were kept at the Experimental Station of the Division of Nutrition and Physiology, Federal Agricultural Research Station Liebefeld-Posieux, Posieux, Freiburg, Switzerland in loose housing systems on straw litter. Cattle used for tissue immunohistochemical analyses were held at USDA, Beltsville, MD in loose housing systems on straw litter. In order to eliminate confounding effects of proinflammatory infection stress on reactive nitrogen oxides status, no animals with fever, clinical signs of illness, and/or requiring therapeutic medication were included in the study.

Calves held in Switzerland were fed colostrum (10% of body weight per day) for 3 days and then whole milk up to the age of 1 month, followed by a commercially available dry nutrient matrix (UFA-200 Natura fluid calf diet; Union

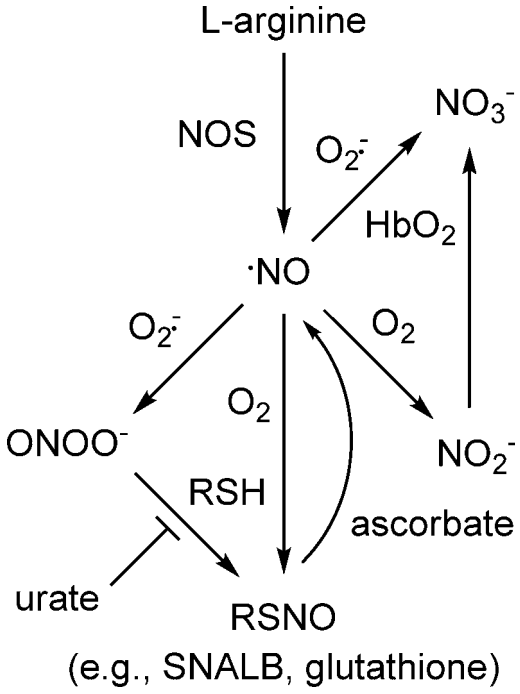

Figure 1. Schematic representation of the possible biochemical interactions between NO, its congeners, thiols, and the plasma antioxidants ascorbate and urate in bovine blood. Because of its charge neutrality, NO produced from the conversion of L-arginine to L-citrulline by the various NOS isoform can diffuse through cell membranes and out of tissues (e.g., from endothelium). In the blood stream, NO can either react with molecular oxygen to form nitrite (NO_2^-) or with superoxide ($O_2^{\cdot-}$) to form peroxynitrite ($ONOO^-$), which either decomposes to nitrate (NO_3^-) or can react with thiols (e.g., albumin, glutathione) to form S-nitrosothiols (RSNO). RSNO are also formed by the reaction of thiols with other reactive nitrogen oxide species (such as N_2O_3) formed during the autoxidation of NO. The plasma antioxidants ascorbate and urate are thought to be involved in the control of the formation and decomposition of RSNO by scavenging $ONOO^-$, supporting NOS function, and promoting the release of NO from RSNO. In red blood cells, oxyhemoglobin (HbO_2) converts diffused NO and taken up NO_2^- to NO_3^-, the major nitrogen oxide species detected in blood plasma. Adapted from Lauer *et al.* (49).

Futter AG, Sursee, Switzerland) mixed in water (100 g/l) typically used in calf husbandry practice and adhering to nutrient standards (26). Calves held in the United States were fed like those in Switzerland. Mature cattle were fed a mixed forage and concentrate ration appropriate for the prevailing physiological state and stage of lactation based on Jans and Kessler (26) for animals held in Switzerland or as per NCR requirements for animals held in the United States.

Single blood samples were taken by jugular venipuncture from each of 19 nontranquilized and minimally restrained calves immediately after birth before feeding colostrum (Day 0), and serially again on Day 1, Day 7, and Day 112 after birth. Blood samples were also taken from 14 healthy, mature, 3- to 5-year-old dairy cows. Blood samples (10 ml each) were collected with evacuated blood collection tubes (Huber, Reinach, Switzerland; containing 1.8 g dipotassium EDTA/l; for biochemical analyses and for blood hematology) fitted with a 20-gauge sterile needle and placed immediately on ice. The hematocrit was measured by standard centrifugation processing, and the pO_2 in venous blood was measured with a portable clinical analyzer (I-STAT Corporation, East Windsor, NJ) as per the manufacturer's recommended procedure. Separation of plasma from blood cells was accomplished by centrifugation (1000 *g* for 20 mins). The resulting plasma was stored protected from light in small aliquots at −80°C until analysis. Subaliquots of blood plasma were prepared for ascorbate and urate analysis by mixing with an equal volume of 10% (w/v) metaphosphoric acid containing 2 m*M* EDTA before freezing.

For age-dependent tissue sample analysis, Holstein male calves at 4 or 24 hrs or 2 weeks after birth ($n = 3$ per time point) were euthanized by intravenous pentobarbital overdose. Tissues from mature cattle were obtained from animals following a standard commercially applied euthanasia protocol at a U.S. federally inspected meat processing plant. Samples of ileum, liver, pancreas, and lung were excised and immersed in a solution of 4% paraformaldehyde in phosphate buffered saline (10 m*M* phosphate and 0.9% NaCl) for fixation for histologic sectioning. After 24 hrs in the paraformaldehyde, tissues were transferred to 70% ethanol and maintained at 4°C until further processed for sectioning for immunohistochemistry analysis. All procedures, including specimen trimming, paraffin embedding, sectioning and placement of tissue specimens on glass slides, were performed by a commercial pathology laboratory (Histoserve, Inc., Germantown, MD) using standard procedures.

Determination of Total Nitrite+Nitrate. Nitrite+nitrate concentrations were determined in plasma samples filtered through precleaned 5 kDa molecular weight cutoff filters (Ultrafree Biomax, Millipore, Bedford, MA) using a modified Griess assay (27). In this assay, nitrate is enzymatically reduced by nitrate reductase, with reducing equivalents provided by a glucose-6-phosphate/glucose-6-phosphate dehydrogenase-driven recycling system, followed by colorimetric detection of nitrite by reaction with Griess reagents. The assay was linear up to a concentration of 0.5 m*M*, with a lower detection limit of ~1 μ*M*.

Determination of Ascorbate and Urate. Ascorbate and urate were measured in metaphosphoric acid-stabilized plasma samples by ion-pairing HPLC, with slight modifications as described (28). Briefly, the sample supernatant was diluted 1:10 with analytical-grade water containing 1 m*M* EDTA and injected onto a 15 × 0.46-cm Supelcosil LC-18-DB column (5 μm particle size, Supelco, Bellefonte, PA), eluted at 1 ml/min with a mobile phase containing 1 volume of acetonitrile and 7 volumes of a solution containing 5 m*M* disodium hydrogen phosphate, 2 m*M* EDTA, and 1.07 m*M* myristyltrimethylammonium bromide, pH adjusted to 5.5 with orthophosphoric acid. The two analytes were monitored by electrochemical detection (Coulochem 5100A detector with a model 5011 analytical

cell, ESA, Inc., Chelmsford, MA) at a potential of +400 mV and quantified by comparison with authentic standards.

Determination of RSNO by Spin Trapping EPR Spectrometry. Plasma RSNO concentrations in samples from 6 animals (plus corresponding number of adults) were determined by spin trapping EPR spectrometry, a recently established specific and validated method (29). In this method, RSNO are decomposed and the NO released captured by the spin trap iron(II) N-methyl-D-glucamine dithiocarbamate (Fe^{2+}-$[MGD]_2$) at high pH. Briefly, ammonium ferrous sulfate (20 m*M*, Sigma) and MGD (100 m*M*, gift from Randox Laboratories, County Antrim, UK) were prepared in deaerated CAPS buffer (0.2 *M*, pH 10.5, Sigma) in evacuated collection tubes and stored on ice until used. The ammonium ferrous sulfate solution (25 μl) was then added to an equal volume of MGD in an evacuated glass vial to produce the spin trap Fe^{2+}-$(MGD)_2$ immediately prior to sample addition. Gas tight syringes and glass vials with a rubber septum in the cap were used to prevent air entering the system. Each biological sample (700 μl) was pretreated with 10 μL of 250 m*M* N-ethyl maleimide for 20 mins at room temperature. An aliquot from the pretreated sample (50 μL) was then added to the spin trap and incubated for 5 mins at room temperature. The samples were analyzed in a WG-LC-11 quartz flat cell using a Jeol FR30 EPR spectrometer. The spectral acquisition parameters were microwave frequency 9.45 GHz, microwave power 20 mW, center field 331.1 mT, sweep width 4 mT, time constant 80 secs, modulation frequency 100 kHz, modulation width 1 mT, and average of three sweeps. RSNO concentrations were calculated by comparing the area of the middle peak of the characteristic triplet signal corresponding to the NO-Fe^{2+}-$(MGD)_2$ spin adduct with a standard curve generated with S-nitrosoglutathione (Axxora Ltd., Nottingham, UK).

Preparation of SNALB. SNALB was synthesized by transnitrosation of bovine albumin with the NO donor SNAP, essentially as described (30). Briefly, bovine serum albumin (BSA, 1 m*M* in 200 m*M* potassium phosphate buffer pH 6.0) was reduced with 10 m*M* dithiothreitol and purified on a PD-10 column equilibrated with 200 m*M* potassium phosphate buffer (pH 8.0) containing 0.2 m*M* EDTA. Reduced BSA was then incubated with a 5 molar excess of SNAP in the same buffer at room temperature. The progression of transnitrosation was followed spectrophotometrically by monitoring the shift in absorbance maxima exhibited by SNAP ($\varepsilon_{590nm} = 47\ M^{-1}\ cm^{-1}$) and NO-BSA ($\varepsilon_{545nm} = 15\ M^{-1}\ cm^{-1}$), respectively. After 30 mins, unreacted SNAP was removed by passing the reaction mixture over a PD-10 column that was equilibrated with potassium phosphate buffer (pH 8.0) containing 0.2 m*M* EDTA. The concentration of SNALB was determined using $\varepsilon_{334nm} = 870\ M^{-1}\ cm^{-1}$ (31). The SNALB preparation contained ~0.6 S-nitroso groups per molecule of BSA.

Analysis of S-Nitrosylated Proteins by Biotin Switch. Putative S-nitrosylated proteins were analyzed using the biotin switch method essentially as described (32). Briefly, 0.2 ml of diluted plasma (adjusted to 0.7 mg protein/ml) was incubated with 0.8 ml of 20 m*M* MMTS in 250 m*M* HEPES-NaOH, 1 m*M* EDTA, 0.1 m*M* neocuproine, pH 7.7 (HEN buffer) containing 2.5% (w/v) sodium dodecyl sulfate for 40 mins at 56°C. Unreacted MMTS was then removed by acetone precipitation (2000 *g* for 10 mins, twice) and the resulting protein pellet resuspended in 0.1 ml HEN buffer. RSNO groups were selectively reduced and labeled by incubation with ascorbate (1 m*M*) and biotin-HPDP (4 m*M*) in dimethylformamide for 1 hr at room temperature. Labeled proteins were then separated on polyacrylamide gels under nonreducing conditions, blotted onto polyvinylidene fluoride membranes, and blocked as described previously (33). Labeled proteins were detected by enhanced chemiluminescence (Super-Signal West Pico, Pierce) using horseradish peroxidase-conjugated neutravidin (1:50,000). Total BSA was detected on the same membrane after stripping and reprobing with 1:5000 mouse monoclonal antibody clone BSA-33 (Sigma).

Analysis of S-Nitrosylated Proteins by Western Blotting. In order to complement and further validate the nitrosylation data obtained with the biotin switch procedure, S-nitrosylated proteins were also analyzed by Western blotting using an antibody directed against SNC. Plasma samples were separated by SDS-PAGE under reducing conditions and blotted onto nitrocellulose. Membranes were incubated overnight with 1:500 rabbit polyclonal anti-SNC (Sigma N-5411) at 4°C and bands visualized by enhanced chemiluminescence detection using an appropriate horseradish peroxidase-labeled secondary antibody. Total BSA was detected as described for the biotin switch method.

Analysis of S-Nitrosylated Proteins, Inducible NOS (iNOS), and Activated Endothelial NOS (eNOS Phosphorylated at Ser1177) in Tissue Sections. Immunohistochemical visualization of protein SNC residues was used as a biomarker for the presence of S-nitrosylated proteins (34) in tissues from calves. Following paraffin removal in xylene and rinsing in 100% ethanol, endogenous peroxidase activity was eliminated by incubating the slides in methanol containing 0.3% hydrogen peroxide for 20 mins. Slides were then rehydrated through graded decreasing levels of ethyl alcohol to pure water. Antigen exposure was enhanced by heating the slides in citrate (pH 6.0) buffer for 15 mins at 70°C, followed by an additional 10-min incubation in TRIS-saline containing 0.05% Triton X-100. Nonspecific binding was blocked by incubating tissue sections in 3% normal rabbit serum (for rat antibody) or 3% horse serum (mouse monoclonal antibodies) in 1% casein-TRIS-saline buffer for 1 hr at room temperature. Rat anti-SNC was applied to tissue section at a 1:400 dilution in the casein-TRIS-saline buffer and incubated overnight at 4°C in a humidified chamber. Positive and negative controls for SNC were established using tissue sections treated with sodium nitrite in HCl or *p*-hydroxymercuric benzoic acid, respectively, as per Gow et al (34). Inducible (type 2) NOS (iNOS) and Ser1177-phosphorylated eNOS (35) were used

as biomarkers for the presence of catalytically active NOS in the tissues from calves. Anti-phospho-eNOS (Ser1177) and anti-iNOS were applied at 1:1000 dilutions, respectively. Following overnight incubation in a humidified chamber at 4°C, slides were further washed three times in TRIS-saline buffer and incubated in sequence with the respective secondary antibody-biotin and strepavidin-HRP complexes as per kit instructions (Vectastain Elite, Vector Laboratories, Burlingame, CA). Color deposition representative of specific antigen localization was resolved with diaminobenzidine (DAB, 150 mg/200 ml TRIS buffer, pH 7.5) substrate for the HRP and nuclear counterstaining accomplished with a 3-min incubation in Carazzi's hematoxylin followed by a 15-min wash in tap water. Cover slips were mounted following dehydration through ethyl alcohol and dipping in xylene. Slides were examined and photographed using an Olympus BX-40 microscope equipped with an Olympus DP-70-CCI camera.

Estimates of tissue antigen content were obtained by digitized automated pixel counting where pixels specific to a range of DAB-substrate color developments were identified and summated. For quantification purposes, five to eight fields for each tissue specimen and each antibody were photographed and digitally analyzed using Image Pro Plus software (Media Cybernetics, Inc., Silver Spring, MD) through a standardized rubric specified to the gradient range of DAB intensities as previously validated and published (36, 37). All relevant tissue samples were batch processed in a single run to eliminate interprocedural daily variation in results. Each section was photographed at full illumination power using the ×40 objective of an Olympus BX-40 microscope. Captured images were equalized in terms of contrast, brightness, and gamma using the software-driven internal best-fit equalization. The intensity of DAB color-specific staining was obtained by defining through color-cube-based segmentation a spectrum-specific range of wavelengths, hues, and intensities that corresponded to those color attributes detectable by the same staining procedure applied to an internal control liver specimen known to contain positive SNC, iNOS, and phospho-eNOS staining. Specificity of staining was further defined in the software application cutoff criteria where object counts lower than a 3-by-3 pixel unit were eliminated and thus defined the criteria for "background." As defined in this manner, this analytical solution was found to be most commonly associated with false negative staining, thus minimizing errors of false positive inclusion through this conservative rubric. This spectral information was filed into a retrievable *.rge format that was subsequently used for analyzing all images. In this fashion, unbiased continuity of analysis across tissue sections was achieved.

Data Analysis. All quantifiable results are reported as means ± SD, unless stated otherwise. Pixel densities of biotin switch or Western blot bands were obtained by densitometric analysis of x-ray films (Fuji SuperRX) and analyzed and compared using Scion Image (Scion Corp., Frederick, MD). With the exception of data derived from immunohistochemical image analysis, for a given variable comparisons between samples collected at different time points were performed by repeated measures ANOVA and Tukey's *post hoc* test using Prism 4 (GraphPad, San Diego, CA). Unpaired ANOVA was used for comparisons with adult parameters. For the immunohistochemical analysis, data were statistically analyzed and compared using an analysis of variance based on mixed modeling procedures (Proc Mixed, SAS, Statistical Analysis System, Cary, NC). Characterization of the relationships between concentrations of biomarkers and age was performed by regression analysis (Proc Reg, SAS) with resulting highest r^2 values used to suggest optimal mathematical fit to either linear first-order regression or quadratic second-order processes.

Results

Ontogenic Changes of Blood Plasma Parameters. Plasma nitrite+nitrate concentrations were high immediately after birth, significantly decreased within the first week of life (>50% on Day 7), and further declined to reach the lowest mean concentrations measured in the samples that were obtained from mature cattle (Table 1). The decrease of nitrite+nitrate on Day 7 and Day 112 was only partially caused by hemodilution; most of the decrease was independent of a change in hematocrit (Table 1). In contrast to nitrite+nitrate, plasma concentrations of both ascorbate and urate had already declined significantly (>50%) between Day 0 and Day 1 (while hematocrit levels remained virtually the same). Ascorbate concentrations decreased further with increasing age and reached a nadir in mature cattle. Concentrations of ascorbate ($r = 0.54$, $P < 0.0001$) and urate ($r = 0.37$, $P < 0.0004$) both positively correlated with overall nitrite+nitrate concentrations.

Like for nitrite+nitrate, the concentrations of plasma RSNO as determined by spin trapping EPR spectrometry were highest immediately after birth and then gradually declined to undetectable levels in adult cattle (Fig. 2). In contrast to nitrite+nitrate, RSNO concentrations were significantly decreased already on Day 1, similar to ascorbate and urate. RSNO concentrations did not significantly correlate with overall nitrite+nitrate concentrations ($n = 30$, $r = 0.33$, $P > 0.05$). When Day 0 plasma samples ($n = 3$) were filtered through 5-kDa cutoff membranes, only 24.7 ± 14.1% was recovered in the low-molecular weight fraction, indicating that most RSNO were protein-bound.

Characterization of S-Nitrosylated Proteins in Blood Plasma. To further characterize the putative S-nitrosylated proteins, we applied the biotin switch method to plasma samples obtained from calves at different ages. The relevant details of the procedure and validation applied to the samples are depicted in Figure 3. The method is based on blocking free thiols with the methylthiolating agent MMTS (Step 1), followed by selective reduction of S-nitrosylated residues to free thiols by ascorbate (Step 2) and

Table 1. Ontogenic Changes in Blood and Blood Plasma Parameters

	Age (days after birth)				
	0 ($n = 19$)	1 ($n = 19$)	7 ($n = 19$)	112 ($n = 19$)	Adult ($n = 14$)
Nitrite+nitrate (μM)	119.5[a] ± 55.4	106.2 ± 47.5	47.5 ± 30.7***[b]	17.7 ± 9.2***	4.1 ± 2.6
Ascorbate (μM)	42.1 ± 20.1	19.1 ± 9.5***	15.3 ± 7.2***	14.4 ± 6.3***	7.9 ± 3.4***
Urate (μM)	56.5 ± 13.9	27.6 ± 8.7***	28.2 ± 9.7***	17.8 ± 4.3***	30.3 ± 15.8***
Hematocrit (%)	0.37 ± 0.05	0.35[c] ± 0.06	0.29 ± 0.06***	0.29 ± 0.04***	0.35 ± 0.02[d]
Protein (g/l)	42.4 ± 2.1	58.3 ± 4.3***	56.2 ± 3.5***	59.5 ± 3.4***	73.3 ± 3.5***
Albumin (g/l)	30.2 ± 1.7	28.8 ± 2.3*	31.7 ± 1.7**	36.7 ± 1.3***	37.0 ± 1.8***,[d]

[a] Values are reported as means ± SD.
[b] Statistical difference to Day 0 was evaluated by repeated measures ANOVA and Tukey's *post hoc* test, except for comparisons of adult parameters, which were done by unpaired ANOVA. *$P < 0.05$; **$P < 0.01$; ***$P < 0.001$.
[c] Values taken from a previous study (42).
[d] Values taken from the literature.

labeling of the newly formed free thiols with the sulfhydryl-specific reagent biotin-HPDP (Step 3) (Fig. 3A). Biotinylated proteins are then detected by peroxidase-labeled streptavidin after electrophoretic separation under reducing conditions and blotting. The specificity of the biotin switch method for S-nitrosylated proteins was established by running native and S-nitrosylated BSA samples (Fig. 3B). While BSA S-nitrosylated with the NO-releasing agent spermine NONOate (BSA + SNO, Lane 2) or SNAP (BSA + SNAP or SNALB, Lane 3) gave a positive band, native BSA (BSA, Lane 1) did not. When this methodology was applied to a plasma sample from a newborn calf (Lane 5), a positive band was detected that comigrated with S-nitrosylated BSA. The band was not detected when the biotin-HPDP step was omitted (Lane 4).

Using the biotin switch method, three major bands between 50 kDa and ~200 kDa were detected in plasma of newborn and mature cattle (Fig. 4A). No S-nitrosylated proteins were observed below 50 kDa, and the two strong positive bands around 250 kDa were determined to be nonspecific phantom bands (and were not always present), most likely as a result of incomplete blockage of the free thiols in these proteins. One of the major bands was detected at an apparent molecular weight of ~55 kDa and comigrated with synthesized SNALB (migration position indicated by an arrow). The bands perfectly overlapped with albumin detected on the same blot (using a monoclonal anti-BSA antibody), strongly suggesting that it is SNALB. A second positive band was detected at a slightly higher molecular weight. Both of these bands appeared to be highest on Day 0, declining to barely detectable levels in adult cattle. The higher molecular weight band was also observed with BSA S-nitrosylated *in vitro* (i.e., synthesized SNALB, data not shown). A third band was detected at 125 kDa. However, this band was only present in plasma samples from Day 1 and mature cattle, but not Day 0 calves.

Suspecting that the 125-kDa band might represent immunoglobulin G (IgG), we subjected plasma samples from Day 0 and Day 1 to immunoglobulin fractionation by Protein-G affinity chromatography before analysis with the biotin switch assay. A representative experiment is shown in Figure 4B. The 125-kDa band normally detected in Day 1 samples (Lane 5) was absent in the nonimmunoglobulin fraction (Lane 4) but recovered in the immunoglobulin fraction (Lane 2), strongly suggesting that the biotin switch-positive band at 125 kDa is S-nitrosylated IgG (SNIgG). Consistent with this interpretation, no 125-kDa band was detected in the immunoglobulin fraction of the Day 0 sample (Lane 1), and SNALB (cf. Fig. 3A) was recovered in the nonimmunoglobulin fraction (Lane 3 and 4).

S-nitrosylated proteins were also analyzed by Western blotting using an antibody against SNC. Similar to the biotin switch method, an immunopositive band (doublet) was detected at an apparent molecular weight of ~60 kDa in plasma from newborns (Fig. 5A) that gradually disappeared with increasing age (see also Fig. 5B). Again, the SNC-positive bands overlapped with albumin detected on the same blot and comigrated with synthesized SNALB (migration position indicated by an arrow). SNC-positive bands at ~25 and 70 kDa that increase with age were also observed.

Tissue Localization of S-Nitrosocysteine in Calves. Based on the immunohistochemical presentation of antigens for SNC, iNOS, and Ser1177-phosphorylated eNOS, a general survey of four tissues from different age calves indicated that the timing and origin of S-nitrosylation differed between tissues (Fig. 6). SNC immunostaining was present in the ileum and liver samples of all calves at 4 hrs after birth and in two out of three calves at 24 hrs after birth, but was largely absent in lung or pancreas of any calves. An occasional diffuse presence of SNC was detected in isolated bronchiolar epithelial cells in two of the three 2-week-old calves. SNC was not present in any sections of pancreas in any calf at 2 weeks of age.

The relationship between the location of enzymes capable of generating NO, specifically iNOS and phosphorylated eNOS, as a precursor to the S-nitrosylation reaction relative to the localization of SNC is depicted in

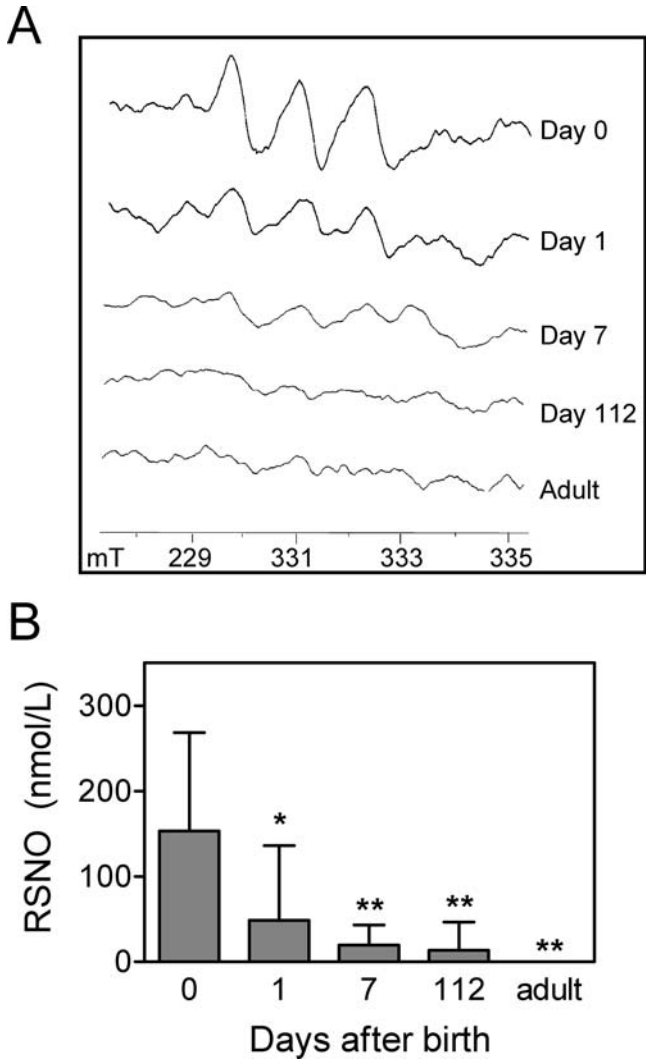

Figure 2. Ontogenic changes of bovine blood plasma RSNO. (A) Representative EPR spectra of blood plasma samples analyzed for RSNO by spin trapping EPR spectrometry obtained from an animal on Day 0, Day 1, Day 7, and Day 112 after birth and an adult animal. Acquisition parameters are stated under Materials and Methods. The receiver gain was 10,000 throughout. (B) Mean ± SD of the RSNO concentration in plasma samples obtained from calves ($n = 6$) on Day 0, Day 1, Day 7, or Day 112 after birth, and adult cows ($n = 6$). Asterisks indicate significant difference compared with Day 0. $^{*}P < 0.05$, $^{**}P < 0.01$.

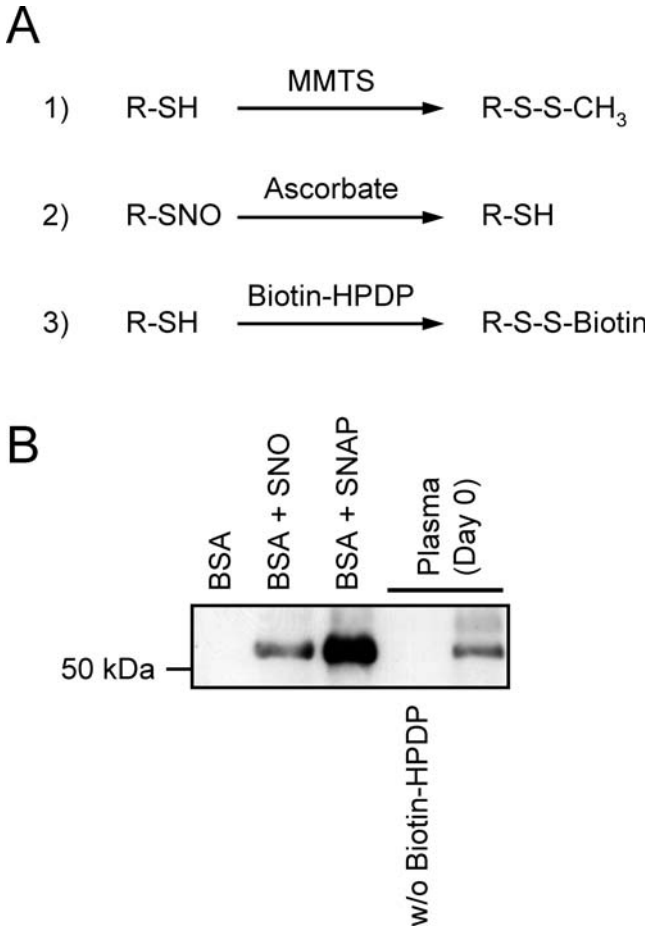

Figure 3. Principle and characterization of the biotin switch method. (A) Basic principles of method: 1) Free thiols (R-SH) are blocked with MMTS to prevent labeling with biotin reagent. 2) Subsequently, S-nitrosothiol (RSNO) groups are selectively reduced by ascorbate to free thiols. 3) Finally, newly formed free thiols are specifically labeled with *N*-[6-(biotinamido)hexyl]-3′-(2'-pyridyldithio) propionamide (biotin-HPDP). (B) Biotin switch method was applied to native bovine serum albumin (BSA, Lane 1), BSA exposed to spermine NONOate (150 μM albumin was incubated with 1 m*M* NO-donor for 4 hrs at 37°C in 100 m*M* potassium phosphate buffer, pH 7.4) (Lane 2), SNALB prepared by transnitrosation with S-nitroso-N-acetylpenicillamine (SNAP, Lane 3), or plasma from a newborn calf (Day 0, Lane 5). Lane 4: same as sample in Lane 5, except that biotin-HPDP was omitted. Biotinylated samples (5 μg protein each) were separated on a 7.5% SDS-polyacrylamide gel under nonreducing conditions, blotted onto a PVDF membrane, and probed for S-nitrosylation with horseradish-conjugated streptavidin (1:50,000) and enhanced chemiluminescence.

Figure 7 for gut and in Figure 8 for liver specimens. The patterns of immunostaining as generated by the development of the DAB-derived color is seen in panels labeled "a." Panels labeled "b" illustrate the DAB color-specific pixels for each "a" figure identified by the image analysis software for each antigen where counted pixels are recolored red and highlighted. Summary statistics for the quantification of pixels for each antigen is presented in Table 2. For the purposes of uniformity in tissue processing, the immunostaining for SNC (as originally performed for Fig. 6) was repeated in a new set of tissue sections from the same animals. In tissue samples of ileum (Fig. 7) it is apparent that SNC, iNOS, and eNOS are present at 4 hrs after birth. Whereas pixel densities associated with SNC and iNOS more than doubled between 4 and 24 hrs after birth (Table 2, $P < 0.05$), tissue levels of eNOS largely remained constant. At 2 weeks after birth tissue levels of antigen for SNC, phosphorylated eNOS, and iNOS decreased to levels 20% or lower (some nondetectable) than those measured in samples from calves at 4 hrs (Table 2, $P < 0.01$). Based on the localization patterns, eNOS was more prominent in the luminal-site cells of villi, while iNOS, especially at 4 hrs, was more centrally positioned. The central positioning of the iNOS and its apparent consolidation in the luminal sides

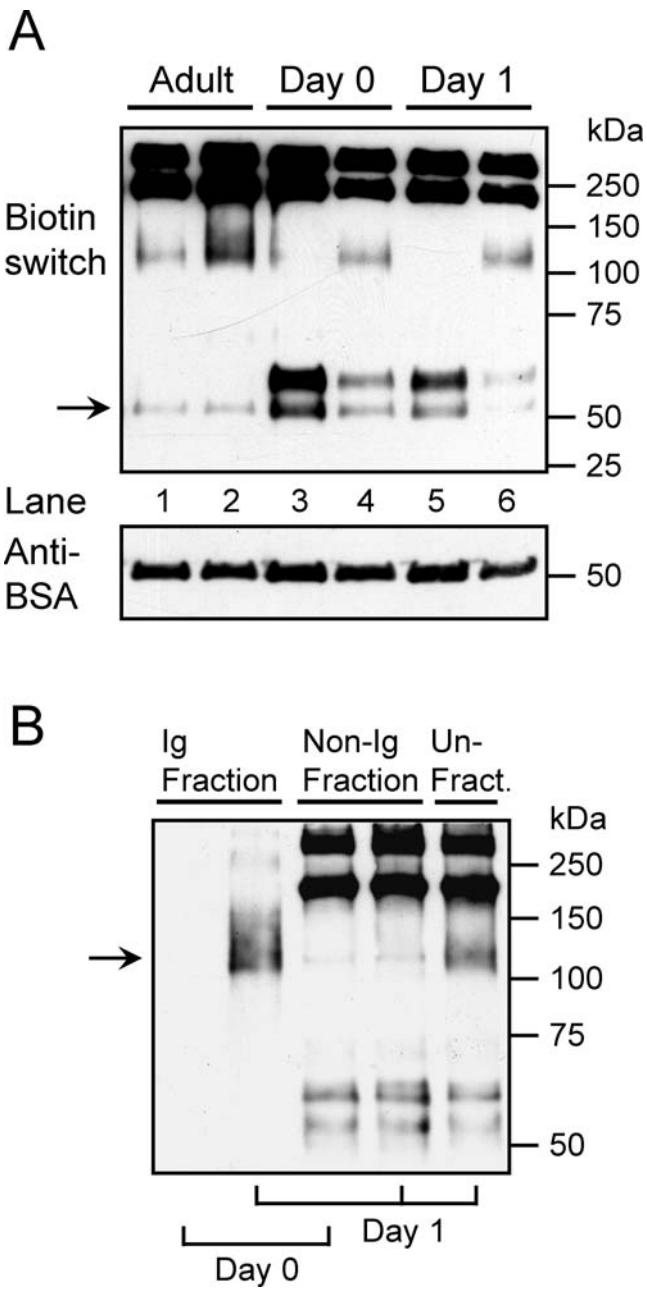

Figure 4. Analysis of S-nitrosylated proteins in bovine blood plasma by biotin switch. (A) Biotin switch method as described in Legend to Figure 2 was applied to plasma samples from two different adult cows (Lanes 1 and 2) and two different neonatal calves on Day 0 (Lanes 3 and 4) and Day 1 (Lanes 5 and 6), respectively. Equal amounts of protein were loaded for each lane. Arrow indicates band comigrating with synthetic SNALB. ns = nonspecific bands. Molecular weights of markers are indicated on right hand side (in kDa). Same blot was reprobed with anti-BSA after stripping. (B) Detection of S-nitrosylated proteins after Protein G affinity chromatography. Plasma samples from a Day 0 (Lanes 1 and 3) and Day 1 (Lanes 2, 4, and 5) animal were subjected to protein G affinity chromatography (50) before analysis by the biotin switch method. To prevent artifactual nitrosylation, nitrite+nitrate was removed from plasma samples by first passing over a PD-10 column equilibrated with binding buffer (20 m*M* sodium phosphate, pH 7.4). The protein fraction was loaded onto a 1-ml HiTrap Protein-G HP column equilibrated with binding buffer and nonimmunoglobulin proteins eluted with 5 ml binding buffer. Immunoglobulins were eluted with 5 ml 0.1 *M* citric acid (pH 2.6) and immediately neutralized with 1 *M* Tris-HCl (pH 9.0). Immunoglobulin (Lanes 1 and 2) and nonimmunoglobulin (flow-through, Lanes 2 and 3) fractions, as well as unfractionated plasma from Day 1 calf (Lane 5), were processed by the biotin switch method as described in Legend to Figure 3, and S-nitrosylated proteins detected with horseradish peroxidase-conjugated streptavidin after separation of proteins under nonreducing conditions. Arrow indicates the migration position of purified IgG.

of the intestinal villi largely mirrored the presentation of SNC.

The SNC, iNOS, and eNOS antigens in the liver were also present immediately after birth. In contrast to the ileal tissue patterns of SNC, liver SNC levels declined between 4 and 24 hrs after birth and remained nondetectable through 2 weeks. The temporal presentation of SNC localized within the liver, however, was not as closely related to that of iNOS and eNOS. Between 4 and 24 hrs after birth, iNOS antigen pixel density increased 5-fold ($P < 0.05$), while phosphorylated eNOS levels remained largely unchanged. At 2 weeks of age tissues showed a marked decrease in overall presentation of all biomarker antigens studied ($P < 0.01$). The majority of cells immunopositive for activated eNOS were largely confined to vascular tissues and discrete cells lining hepatic sinuses. Residual iNOS staining at 2 weeks of age was confined to a few dispersed hepatocytes also near central venous areas, few vascular cells, and some select cells interspersed between hepatocytes and resembling (by nuclear outline or relative size) infiltrating monocytes or resident Kupffer cells. Discrete punctate immunostaining for SNC in the liver was architecturally structured in regions mainly juxtaposed in proximity to the central vein and other vascular areas. At 2 weeks of age, and within the limits of the sensitivity of the method, there was no evidence of SNC being present in the observed tissue regions of the liver.

Discussion

In a previous study we demonstrated that plasma concentrations of nitrite+nitrate were extremely elevated in calves at birth. Furthermore, these high concentrations were not the result of ingestion of the nitrite+nitrate from first colostrums (22). The significance of this observation suggested that the levels of nitrite+nitrate measured must have originated from an activation of the NOS axis during this transition period resulting in the endogenous production of NO. As an outgrowth of this initial observation, the present study was undertaken to define and characterize how elements of the NOS axis beyond the fundamental changes in NO and nitrite+nitrate interact in the neonate during this critical transition period. The major findings of the present study regarding the NO axis are (i) that the neonatal period in the bovine species is characterized by elevated circulating levels of RSNO, in particular protein conjugates of S-nitrosylated albumin and IgG, (ii) the change in RSNO adducts is tightly correlated with, but differentially affected by, ascorbate and urate changes, and (iii) tissue presentation of the S-nitrosylation reaction marker SNC in the ileum and

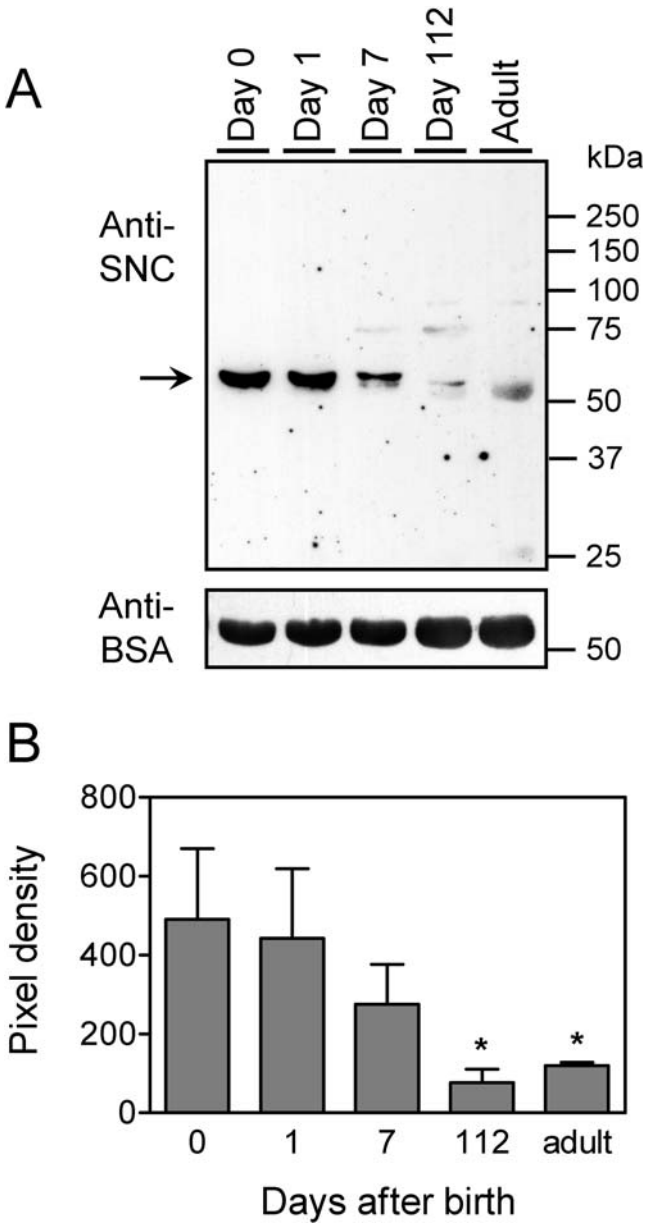

Figure 5. Analysis of S-nitrosylated proteins in bovine blood plasma by Western blotting. (A) Plasma samples obtained at Day 0, Day 1, Day 7, Day 112, and in an adult animal were separated on a 10% SDS-polyacrylamide gel under reducing conditions and blotted proteins probed for S-nitrosylated cysteine residues as described in "Materials and Methods." The blot was reprobed for total albumin after stripping the membrane. (B) Densitometric evaluation of SNALB band. Results represent mean data ± SEM from four calves and corresponding number of adult cattle. Asterisks indicate significant difference to Day 0. *$P < 0.05$.

liver (but not pancreas or lung) can be linked to the ontogenic development and expression of both iNOS and activated eNOS. The development and remission of immunostaining patterns for SNC was dynamic with antigen presence in the villi initiating in the central villus region and condensing in the periphery within hours. This was accompanied by age-related decreases in SNC immunostaining in vascular tissue regions.

The ultrafiltration experiments revealed that most (>75%) of the RSNO detected in plasma samples of newborns was recovered in the protein fraction. The biotin switch- and Western blot-based results with anti-SNC are consistent with SNALB being the major S-nitrosylated protein in bovine blood plasma. Furthermore, the putative band was tracked in two different but complementary biochemical procedures and determined to have followed separation mobility characteristics as defined by synthesized SNALB. These data are also consistent with data from other mammals, in which albumin was the major RSNO in blood plasma (15, 17), most likely because it is the major free thiol in this compartment and readily amenable to S-nitrosylation (17). Like total RSNO, SNALB levels also declined with increasing age. To our knowledge, this is the first report that documents the presence of SNALB in the circulation of healthy cattle. Furthermore, the results of this study characterize the fundamental nature of the age-related decline in RSNO as measured by the sensitive EPR spin trapping technique, evident early in life, which parallels the pattern of change in ascorbate and urate. Interestingly, the pattern of decline in nitrite+nitrate was not directly correlated to ascorbate, urate, or RSNO, supporting the premise that there exist distinct functions in the actions of the various NOS axis components. As can be seen in Figure 9, if concentrations of the various biomarkers for a given day are represented as a percentage of the value on Day 0 (day of birth) and are mathematically regressed on time from Day 0 through Day 7 after birth, one observes that the line describing the decline in nitrite+nitrate concentration had a best fit to a linear function. Conversely, however, lines describing concentration decreases over time for ascorbate, urate, and RSNO were more accurately described as quadratic functions, with the greatest concentration drops occurring within the first day of life. One must be cautious not to overinterpret correlation data. However, the data clearly indicate that in the calf the components of the NOS axis associated with ascorbate, RSNO, and urate must be considered potentially a cluster of more rapidly responding axis components than other elements associated with nitrite+nitrate: for the three variables, ascorbate, RSNO, and urate, the concentrations measured on Day 1 were all significantly lower than those measured on Day 0, whereas the concentrations of nitrite+nitrate measured on Day 0 and Day 1 were similar. In fact, if the data regressions for ascorbate, RSNO, and urate variable concentrations are performed for data on Day 1 through Day 112, one can observe that the slopes of the lines between Day 1 and Day 112 are not different from 0, whereas the slope of the nitrite+nitrate line is still negative, significantly different from 0, and linear. The interpretation, however, still remains complex. Given that the change in RSNO concentrations over time from the EPR spin-trapping technique were not exactly mirrored by the changes in SNC proteins quantified over time by Western blot following electrophoretic separation, one can surmise that the kinetics of generation

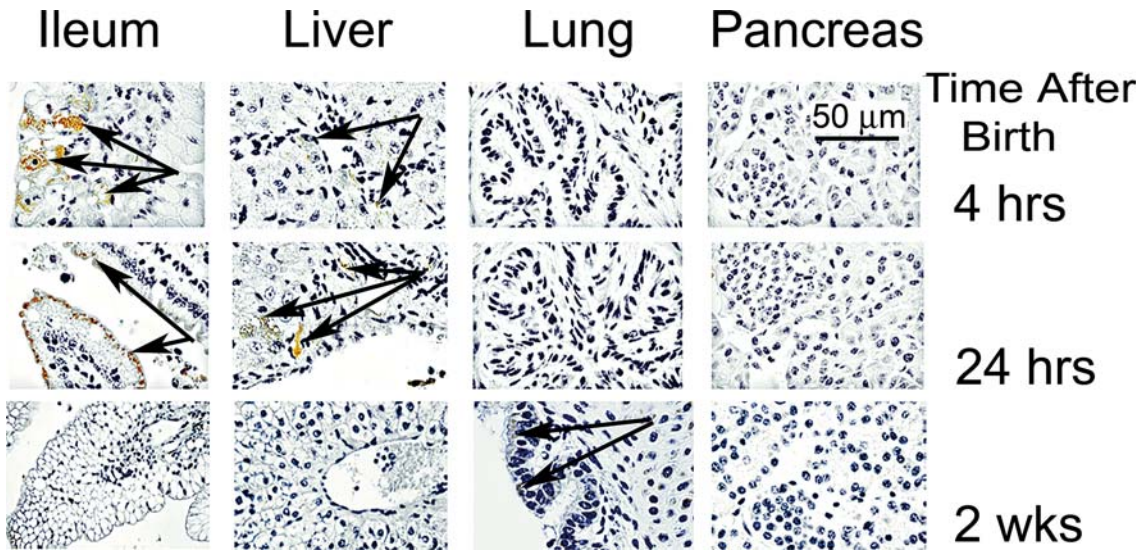

Figure 6. Comparison between tissues (gut, liver, lung, and pancreas) for the immunohistochemical presence of nitrosylated tissue proteins in different aged calves as detected by localization of S-nitrosocysteine antigen (indicated by arrows). The red pixels were generated by the image analysis software for DAB-specific coloration and used for antigen density analysis as per Refs. 36 and 37. Nuclei are stained blue.

and availability release of NO as derived from the many RSNO species differs by source.

These relationships begin to crystallize within the concept that the functionality and purpose of NO *per se* can be separated logically according to the generated source:

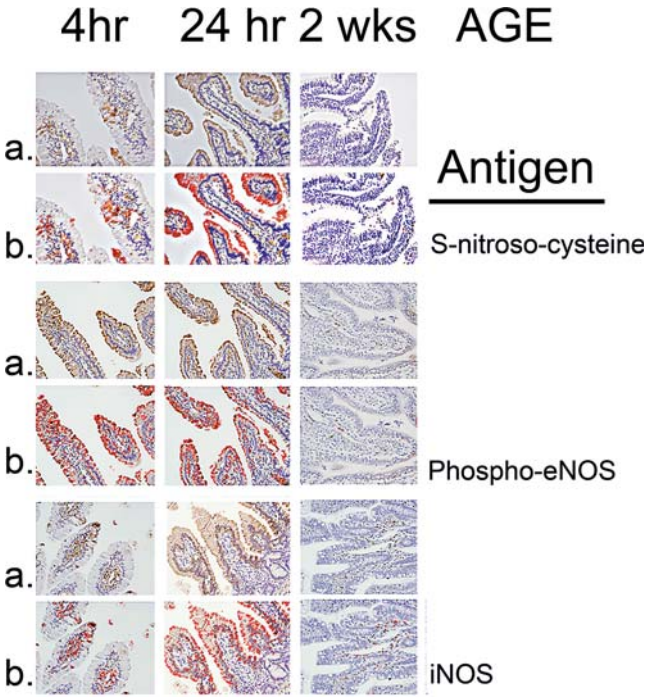

Figure 7. Immunohistochemical localization of SNC, Ser1177-phosphorylated eNOS, and iNOS in ileum obtained from calves at 4 and 24 hrs and 2 weeks after birth. Panels labeled "a" represent actual immunostaining visualized with oxidation of DAB by horseradish peroxidase. Panels labeled "b" are the output from the image analysis software through which processing DAB color-specific pixels are identified and represented as counted by the substituted intense red color.

localized *de novo* production versus regeneration/release from RSNO. The *de novo* generation is more aligned with recognized acutely produced, spatially limited, and diffusion-dependent processes, in contrast to those processes affected by NO derived over longer periods of time and distance from the release of NO from RSNO and S-nitrosylated proteins such as SNALB, as might occur in very localized regional tissue environments. Furthermore, we begin to see elements of fine-tuning of the directed actions of NO in different tissues if we consider that the local presence of ascorbate and uric acid modulate the production and rerelease of NO from SNALB (24, 25, 38, 39), while aberrant protein tyrosine nitration may be avoided by the scavenging of peroxynitrite by urate (25). Finally, one must also acknowledge the potential contribution of a maturation of the metabolic axis wherein the metabolic fate and use of substrate arginine becomes further subdivided within the urea cycle, presently known to significantly compete with and to some extent modulate the NO axis (23, 40, 41). To this end, recent data on suckling neonatal piglets have demonstrated that developmental maturation of the urea cycle is needed to accommodate detoxification of ammonia, and where animals are deficient in arginine (substrate for both NOS and urea cycle enzymes) there can develop a critical imbalance between physiological systems necessary for metabolic homeostasis (41). In contrast to these data obtained using the neonatal pig model (41), our data from the calf may in fact be more revealing in regard to exactly how dynamic the change in NO axis activities can be as well as the interaction between the NOS compartment and the urea cycle when one compares how much more the changes in the measured variables are in the calf compared to the pig.

In addition to albumin, IgG is obviously also a target of

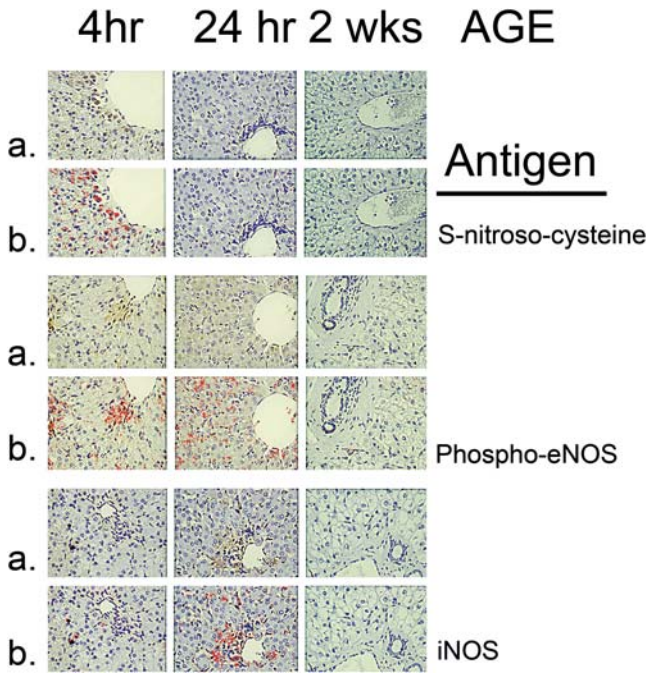

Figure 8. Immunohistochemical localization of SNC, Ser1177-phosphorylated eNOS, and iNOS in liver tissue obtained from calves at 4 and 24 hrs and 2 weeks after birth. Panels labeled "a" represent actual immunostaining visualized with oxidation of DAB by horseradish peroxidase. Panels labeled "b" are the output from the image analysis software through which processing DAB color-specific pixels are identified and represented as counted by the substituted intense red color.

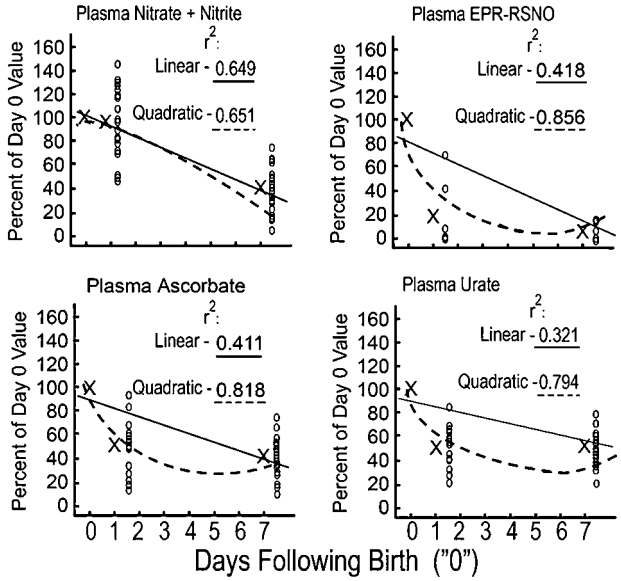

Figure 9. When data for ascorbate, nitrite+nitrate, RSNO (determined by the EPR spin trapping technique), and urate were normalized as a percentage of the initial values on Day 0 of life and mathematically regressed on age, it was apparent that the concentration declines for ascorbate, RSNO, and urate follow exponential decay kinetics whereas that for nitrite+nitrate was linear.

S-nitrosylation. Thus, a biotin switch-positive band was detected that comigrated with purified IgG, was selectively retained by Protein G, and was absent in samples of calves that had not received any colostrum (containing IgG) yet. Interestingly, the levels of the putative SNIgG remained elevated with age, despite the fact that circulating levels of nitrite+nitrate and RSNO, as well as those of IgG (42) are lower in adult cows compared to neonatal calves. A similar pattern of change was observed for two bands at ~25 and 70 kDa in the Western blot experiment. Whether these bands represent IgG (although consistent by molecular weight) is presently unknown. Our results warrant IgG to be considered as an additional target for S-nitrosylation *in vivo*.

This paper is also the first to describe the contemporary localization of SNC, iNOS, and eNOS as a function of neonatal age. Taken together, our data clearly show that the neonatal period in the bovine species is characterized by highly elevated and coordinated NO-generating and nitrosylation events as compared with obvious lower levels of these biomarkers in healthy older cattle. Illustrating how critical (and dynamic) the timing of sampling is in the interpretation of results, SNC-immunostaining was present in ileum and liver tissues of all calves studied as early as 4 hrs after birth. Furthermore, SNC immunostaining increased 2-fold in the ileum between 4 and 24 hrs, while during the same time it significantly decreased in the liver. The data are

Table 2. Mean Antigen Pixel Density in Photomicrographs of Ileum and Liver Tissue As a Function of Calf Age As Processed for Digitized Image Analysis

Antigen	Tissue	4 hrs after birth	24 hrs after birth	2 wks after birth
S-nitrosothiol	Ileum	836 ± 237[c]	2013 ± 632*	131 ± 54**
	Liver	1156 ± 433	39 ± 20 (N.D.)[d]***	16 ± 12 (N.D.)***
Phospho-eNOS[a]	Ileum	2983 ± 1027	3319 ± 1010	224 ± 88**
	Liver	1708 ± 886	1223 ± 413	145 ± 99**
iNOS[b]	Ileum	1024 ± 357	2268 ± 227*	374 ± 123**
	Liver	226 ± 80	1139 ± 288*	5 ± 5 (N.D.)**

[a] Ser-1177-phosphorylated endothelial NOS, activated.
[b] Inducible, Type-2 NOS.
[c] Data represent mean pixel density (± SEM) for a specific antigen , $n = 3$ calves per group as derived from digitized analysis of images from Figures 6 and 7.
[d] N.D., nondetectable (not able to resolve from background scatter).
* $P < 0.05$ versus 4 hrs; ** $P < 0.01$ versus 4 hrs; *** $P < 0.005$.

consistent with the idea that SNC, phosphorylated eNOS, and iNOS antigen densities differ between many tissues. The data likely reflect the physiological need for the NO axis to participate in stabilizing the transitions associated with life independent of the placenta that occur at birth. In many images of liver tissue we noticed an abundance of low-density matrix immunostaining positive for the antibody against SNC, eliminated with absorption control methods or higher dilutions of primary antibody and not related to endogenous liver biotin or second antibody or avidin-biotin enhancement protocols. This can be interpreted to suggest that S-nitrosylated proteins like SNALB are rapidly exported from the liver into the circulation. This could likely account for observed differences in SNC staining in the liver over time and also possibly serve to underscore the difference in localized function of RSNO/SNC/SNALB in the liver (as a generating source) versus the gut (present for localized regulatory purposes). Furthermore, with regard to changes in pixel density in the gut as a function of time after birth, some of the quantified changes in the biomarker antigens may also be affected by a functional condensation or accumulation of NO-modified (SNC) or NO-generating (iNOS, phosphorylated eNOS) proteins. This may in fact be what is occurring where pattern changes develop that appear consistent with the concept that pixel density locations change from a rather diffuse pattern more centralized in the villi at 4 hrs to a tight granular pattern peripherally located at the luminal side of villus cells. Although beyond the scope of the intent here, if specific image analysis sharpening and Gaussian curve filters (available in the image analysis software used herein) are applied to the ileum figures to increase resolution of SNC pixels, it becomes apparent that between 4 and 24 hrs after birth there are more antigen pixels present in more clusters located at the margins of the villi, further supporting the notion that this biomarker probably undergoes intracellular transport and possible localized packaging once formed.

The presence of high plasma concentrations of nitrite+nitrate and RSNO at birth is consistent with a large activation of NOS-mediated conversion of arginine to NO. Immunohistochemical evidence presented here further suggests that at least the two major NOS forms, iNOS and activated (Ser1177-phosphorylated) endothelial (eNOS), are present at a near-birth time period (4 hrs after birth). Enhanced formation of NO (19) and RSNO (43) have been proposed to be important for postnatal adaptation of pulmonary circulation in humans. Urinary nitrite+nitrate excretion is elevated in preterm infants compared to full-term infants (44, 45), and plasma levels of nitrite+nitrate are higher in asphyxiated or oxygen-deprived newborns compared to infants born without asphyxia (46), suggesting that enhanced NO formation plays an important role in the neonatal response to hypoxia.

The perinatal period is a time of significant transition stress during which the needs of the infant are transferred from their maternocentric origin to the infant itself. The postnatal period requires robust homeostatic rearrangements, and dynamic structure-function relationships must be properly developed in order for respiration, metabolism and immune defense to successfully establish. The present data are consistent with the concept that RSNO may provide a stable form of NO reserves for the neonate necessary for primary immunodefense in the gut and perhaps associated with the prevention of gut ischemia, a significant concern of neonatologists particularly where the potential for sepsis may be present (4). Of special concern are premature infants wherein the extreme upregulation of NO generation by iNOS in necrotizing enterocolitis far overrides the beneficial level of localized increased NO generated by the lower output eNOS pathway needed for vascular regulation (47, 48). Though beyond the scope of the present paper, changes in management procedures involving improved and stabilizing enteral nutrition, including colostrum ingestion by the infant, has contributed to a significant improved clinical outcome of prematurely born children (47, 48). The involvement and role of active nitrosylation of ingested IgG remains to be elucidated here. Furthermore, comparatively rapid changes in the tissue content of these molecules is also consistent with their purported role as intermediaries of signal transduction processes in which nitrosylation and denitrosylation (2, 3) of proteins modulates the pathways important to intermediary metabolism (3). The temporal changes in plasma nitrite+nitrate, RSNO, and S-nitrosylated proteins and the tissue distribution of NOS isoforms suggest that the NO cascade is important to the survival of the neonate and is highly coordinated.

In summary, the results of the present study demonstrate that the perinatal period in the bovine species is characterized by obviously marked endogenous NO formation (22) and that the elevated nitrite+nitrate status is accompanied by increased RSNO levels (among which SNALB and SNIgG are the major S-nitrosylated proteins). Because of high endogenous nitrite+nitrate and RSNO levels at birth, the bovine species is a particularly interesting model to study the role of NO and its congeners in neonatal physiology.

We thank Corinne Siegenthaler for technical assistance with biochemical analyses, Sidney G. Shaw for useful discussions, and Stanislaw Kahl for critical evaluation of the manuscript.

1. Sasidharan P. Role of corticosteroids in neonatal blood pressure homeostasis. Clin Perinatol 25:723–740, xi, 1998.
2. Gow AJ, Chen Q, Hess DT, Day BJ, Ischiropoulos H, Stamler JS. Basal and stimulated protein S-nitrosylation in multiple cell types and tissues. J Biol Chem 277:9637–9640, 2002.
3. Gow AJ, Farkouh CR, Munson DA, Posencheg MA, Ischiropoulos H. Biological significance of nitric oxide-mediated protein modifications. Am J Physiol Lung Cell Mol Physiol 287:L262–L268, 2004.
4. Huang Y, Shao XM, Neu J. Immunonutrients and neonates. Eur J Pediatr 162:122–128, 2003.

5. Adan D, La Gamma EF, Browne LE. Nutritional management and the multisystem organ failure/systemic inflammatory response syndrome in critically ill preterm neonates. Crit Care Clin 11:751–784, 1995.
6. Cylwik D, Mogielnicki A, Buczko W. L-arginine and cardiovascular system. Pharmacol Rep 57:14–22, 2005.
7. Shaul PW. Regulation of vasodilator synthesis during lung development. Early Hum Dev 54:271–294, 1999.
8. MacRitchie AN, Jun SS, Chen Z, German Z, Yuhanna IS, Sherman TS, Shaul PW. Estrogen upregulates endothelial nitric oxide synthase gene expression in fetal pulmonary artery endothelium. Circ Res 81:355–362, 1997.
9. Hascoet JM, Fresson J, Claris O, Hamon I, Lombet J, Liska A, Cantagrel S, Al Hosri J, Thiriez G, Valdes V, Vittu G, Egreteau L, Henrot A, Buchweiller MC, Onody P. The safety and efficacy of nitric oxide therapy in premature infants. J Pediatr 146:318–323, 2005.
10. Thibeault DW. The precarious antioxidant defenses of the preterm infant. Am J Perinatol 17:167–181, 2000.
11. Alberti-Fidanza A, Burini G, Perriello G. Total antioxidant capacity of colostrum, and transitional and mature human milk. J Matern Fetal Neonatal Med 11:275–279, 2002.
12. Kelm M. Nitric oxide metabolism and breakdown. Biochim Biophys Acta 1411:273–289, 1999.
13. Ignarro LJ, Lippton H, Edwards JC, Baricos WH, Hyman AL, Kadowitz PJ, Gruetter CA. Mechanism of vascular smooth muscle relaxation by organic nitrates, nitrites, nitroprusside and nitric oxide: evidence for the involvement of S-nitrosothiols as active intermediates. J Pharmacol Exp Ther 218:739–749, 1981.
14. Mellion BT, Ignarro LJ, Myers CB, Ohlstein EH, Ballot BA, Hyman AL, Kadowitz PJ. Inhibition of human platelet aggregation by S-nitrosothiols. Heme-dependent activation of soluble guanylate cyclase and stimulation of cyclic GMP accumulation. Mol Pharmacol 23:653–664, 1983.
15. Stamler JS, Simon DI, Osborne JA, Mullins ME, Jaraki O, Michel T, Singel DJ, Loscalzo J. S-nitrosylation of proteins with nitric oxide: synthesis and characterization of biologically active compounds. Proc Natl Acad Sci U S A 89:444–448, 1992.
16. Keaney JF Jr., Simon DI, Stamler JS, Jaraki O, Scharfstein J, Vita JA, Loscalzo J. NO forms an adduct with serum albumin that has endothelium-derived relaxing factor-like properties. J Clin Invest 91: 1582–1589, 1993.
17. Rafikova O, Rafikov R, Nudler E. Catalysis of S-nitrosothiols formation by serum albumin: the mechanism and implication in vascular control. Proc Natl Acad Sci U S A 99:5913–5918, 2002.
18. Minamiyama Y, Takemura S, Inoue M. Albumin is an important vascular tonus regulator as a reservoir of nitric oxide. Biochem Biophys Res Commun 225:112–115, 1996.
19. Biban P, Zangardi T, Baraldi E, Dussini N, Chiandetti L, Zacc F. Mixed exhaled nitric oxide and plasma nitrites and nitrates in newborn infants. Life Sci 68:2789–2797, 2001.
20. Colnaghi M, Condo V, Pugni L, Fumagalli M, Mosca F. Endogenous nitric oxide production in the airways of preterm and term infants. Biol Neonate 83:113–116, 2003.
21. Levy M, Maurey C, Dinh-Xuan AT, Vouhe P, Israel-Biet D. Developmental expression of vasoactive and growth factors in human lung. Role in pulmonary vascular resistance adaptation at birth. Pediatr Res 57:21R–25R, 2005.
22. Blum JW, Morel C, Hammon HM, Bruckmaier RM, Jaggy A, Zurbriggen A, Jungi T. High constitutional nitrate status in young cattle. Comp Biochem Physiol A Mol Integr Physiol 130:271–282, 2001.
23. Lerzynski G, Suschek CV, Kolb-Bachofen V. In hepatocytes the regulation of NOS-2 activity at physiological l-arginine levels suggests a close link to the urea cycle. Nitric Oxide 14:300–308, 2006.
24. Gandley RE, Tyurin VA, Huang W, Arroyo A, Daftary A, Harger G, Jiang J, Pitt B, Taylor RN, Hubel CA, Kagan VE. S-nitrosoalbumin-mediated relaxation is enhanced by ascorbate and copper: effects in pregnancy and preeclampsia plasma. Hypertension 45:21–27, 2005.
25. Kuzkaya N, Weissmann N, Harrison DG, Dikalov S. Interactions of peroxynitrite with uric acid in the presence of ascorbate and thiols: implications for uncoupling endothelial nitric oxide synthase. Biochem Pharmacol 70:343–354, 2005.
26. Jans F, Kessler J. Fütterungsempfehlungen für Wiederkäuer. Eidgenössische Forschungsanstalt für Nutztiere, Posieux, Switzerland. Zollikofen, Switzerland: Landwirtschaftliche Lehrmittelzentrale, 1999.
27. Verdon CP, Burton BA, Prior RL. Sample pretreatment with nitrate reductase and glucose-6-phosphate dehydrogenase quantitatively reduces nitrate while avoiding interference by NADP+ when the Griess reaction is used to assay for nitrite. Anal Biochem 224:502–508, 1995.
28. Barja de Quiroga G, Lopez-Torres M, Perez-Campo R, Rojas C. Simultaneous determination of two antioxidants, uric and ascorbic acid, in animal tissue by high-performance liquid chromatography. Anal Biochem 199:81–85, 1991.
29. Rocks SA, Davies CA, Hicks SL, Webb AJ, Klocke R, Timmins GS, Johnston A, Jawad AS, Blake DR, Benjamin N, Winyard PG. Measurement of S-nitrosothiols in extracellular fluids from healthy human volunteers and rheumatoid arthritis patients, using electron paramagnetic resonance spectrometry. Free Radic Biol Med 39:937–948, 2005.
30. Barnett DJ, McAninly J, Williams DLH. Transnitrosation between nitrosothiols and thiols. J Chem Soc Perkin Trans 2:1131–1133, 1994.
31. Meyer DJ, Kramer H, Ozer N, Coles B, Ketterer B. Kinetics and equilibria of S-nitrosothiol-thiol exchange between glutathione, cysteine, penicillamines and serum albumin. FEBS Lett 345:177–180, 1994.
32. Jaffrey SR, Erdjument-Bromage H, Ferris CD, Tempst P, Snyder SH. Protein S-nitrosylation: a physiological signal for neuronal nitric oxide. Nat Cell Biol 3:193–197, 2001.
33. Girault I, Karu AE, Schaper M, Barcellos-Hoff MH, Hagen T, Vogel DS, Ames BN, Christen S, Shigenaga MK. Immunodetection of 3-nitrotyrosine in the liver of zymosan-treated rats with a new monoclonal antibody: comparison to analysis by HPLC. Free Radic Biol Med 31:1375–1387, 2001.
34. Gow AJ, Davis CW, Munson D, Ischiropoulos H. Immunohistochemical detection of S-nitrosylated proteins. Methods Mol Biol 279:167–172, 2004.
35. Dimmeler S, Fleming I, Fisslthaler B, Hermann C, Busse R, Zeiher AM. Activation of nitric oxide synthase in endothelial cells by Akt-dependent phosphorylation. Nature 399:601–605, 1999.
36. Elsasser TH, Kahl S, MacLeod C, Nicholson B, Sartin JL, Li C. Mechanisms underlying growth hormone effects in augmenting nitric oxide production and protein tyrosine nitration during endotoxin challenge. Endocrinology 145:3413–3423, 2004.
37. Daniel JA, Elsasser TH, Martinez A, Steele B, Whitlock BK, Sartin JL. Interleukin-1beta and tumor necrosis factor-alpha mediation of endotoxin action on growth hormone. Am J Physiol Endocrinol Metab 289:E650–E657, 2005.
38. Scorza G, Pietraforte D, Minetti M. Role of ascorbate and protein thiols in the release of nitric oxide from S-nitroso-albumin and S-nitroso-glutathione in human plasma. Free Radic Biol Med 22:633–642, 1997.
39. Trujillo M, Alvarez MN, Peluffo G, Freeman BA, Radi R. Xanthine oxidase-mediated decomposition of S-nitrosothiols. J Biol Chem 273: 7828–7834, 1998.
40. Silva MA, Richards DA, Bramhall SR, Adams DH, Mirza DF, Murphy N. A study of the metabolites of ischemia-reperfusion injury and selected amino acids in the liver using microdialysis during transplantation. Transplantation 79:828–835, 2005.
41. Flynn NE, Knabe DA, Mallick BK, Wu G. Postnatal changes of plasma amino acids in suckling pigs. J Anim Sci 78:2369–2375, 2000.
42. Egli CP, Blum JW. Clinical, haematological, metabolic and endocrine traits during the first three months of life of suckling simmentaler calves

held in a cow-calf operation. Zentralbl Veterinarmed A 45:99–118, 1998.

43. Gaston B, Fry E, Sears S, Heroman WM, Ignarro L, Stamler JS. Umbilical arterial S-nitrosothiols in stressed newborns: role in perinatal circulatory transition. Biochem Biophys Res Commun 253:899–901, 1998.
44. Tsukahara H, Hiraoka M, Hori C, Tsuchida S, Hata I, Nishida K, Kikuchi K, Sudo M. Urinary nitrite/nitrate excretion in infancy: comparison between term and preterm infants. Early Hum Dev 47:51–56, 1997.
45. Dzik JM, Dobrzanska A, Gruszfeld D, Walajtys-Rode E. Nitric oxide metabolites in the urine of full-term and preterm infants. Pediatr Int 44: 368–375, 2002.
46. Fulia F, Gitto E, Cuzzocrea S, Reiter RJ, Dugo L, Gitto P, Barberi S, Cordaro S, Barberi I. Increased levels of malondialdehyde and nitrite/nitrate in the blood of asphyxiated newborns: reduction by melatonin. J Pineal Res 31:343–349, 2001.
47. Neu J, Weiss MD. Necrotizing enterocolitis: pathophysiology and prevention. J Parenter Enteral Nutr 23:S13–S17, 1999.
48. Ford H, Watkins S, Reblock K, Rowe M. The role of inflammatory cytokines and nitric oxide in the pathogenesis of necrotizing enterocolitis. J Pediatr Surg 32:275–282, 1997.
49. Lauer T, Kleinbongard P, Kelm M. Indexes of NO bioavailability in human blood. News Physiol Sci 17:251–255, 2002.
50. Aybay C, Imir T. Development of a rapid, single-step procedure using protein G affinity chromatography to deplete fetal calf serum of its IgG and to isolate murine IgG1 monoclonal antibodies from supernatants of hybridoma cells. J Immunol Methods 233:77–81, 2000.